Detection capability for native defect by the actinic blank inspection

EUVL Infrastructure development Center, Inc.
Takeshi Yamane
Lasertec Corporation
Tomohisa Ino, Tomohiro Suzuki, Hiroki Miyai, Kiwamu Takehisa, Haruhiko Kusunose

Outline

1. Introduction
2. Defects detected by ABI
3. Not detected defects by ABI
4. Summary

Outline

1. **Introduction**
2. Defects detected by ABI
3. Not detected defects by ABI
4. Summary

Actinic blank inspection (ABI) tools

MIRAI-tool
(Full-field inspection prototype)

Developed by Selete and EIDEC
Available since August, 2008

This work

HVM ABI prototype

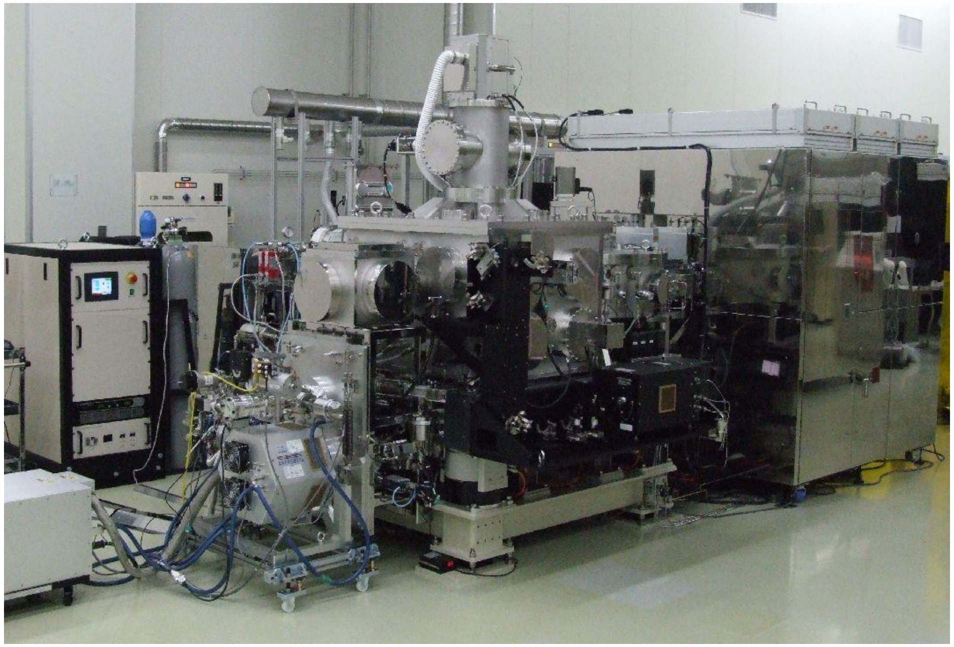

Developed by Lasertec and EIDEC
Available since December, 2012

Schema of Actinic Blank Inspection

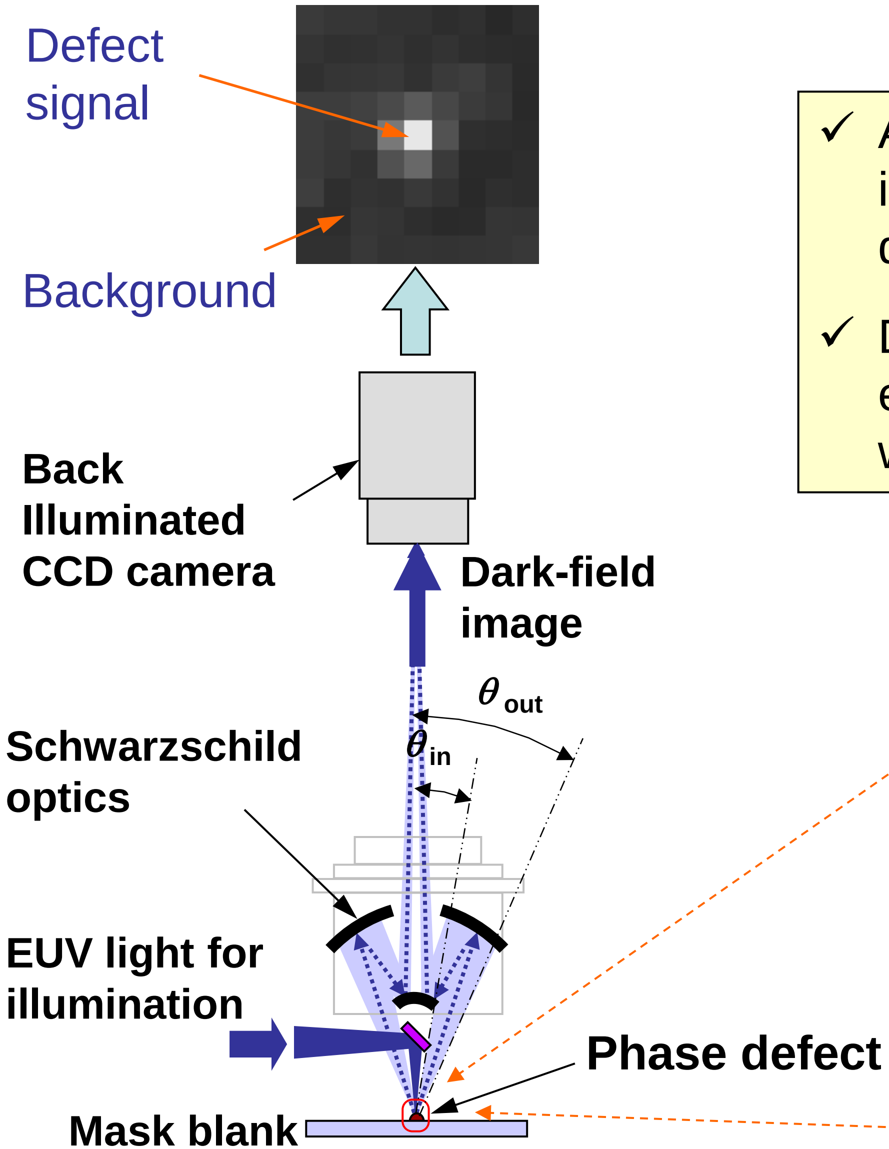

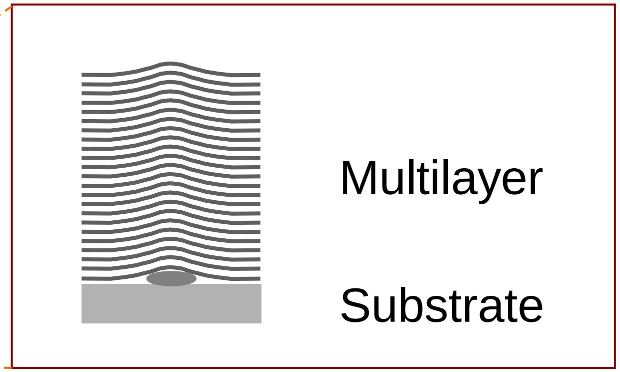

- ✓ Actinic Blank Inspection (ABI) is effective especially for phase defect buried in multilayer
- ✓ Dark field imaging optics enables high defect sensitivity with high throughput

Defect sensitivity of HVM ABI prototype

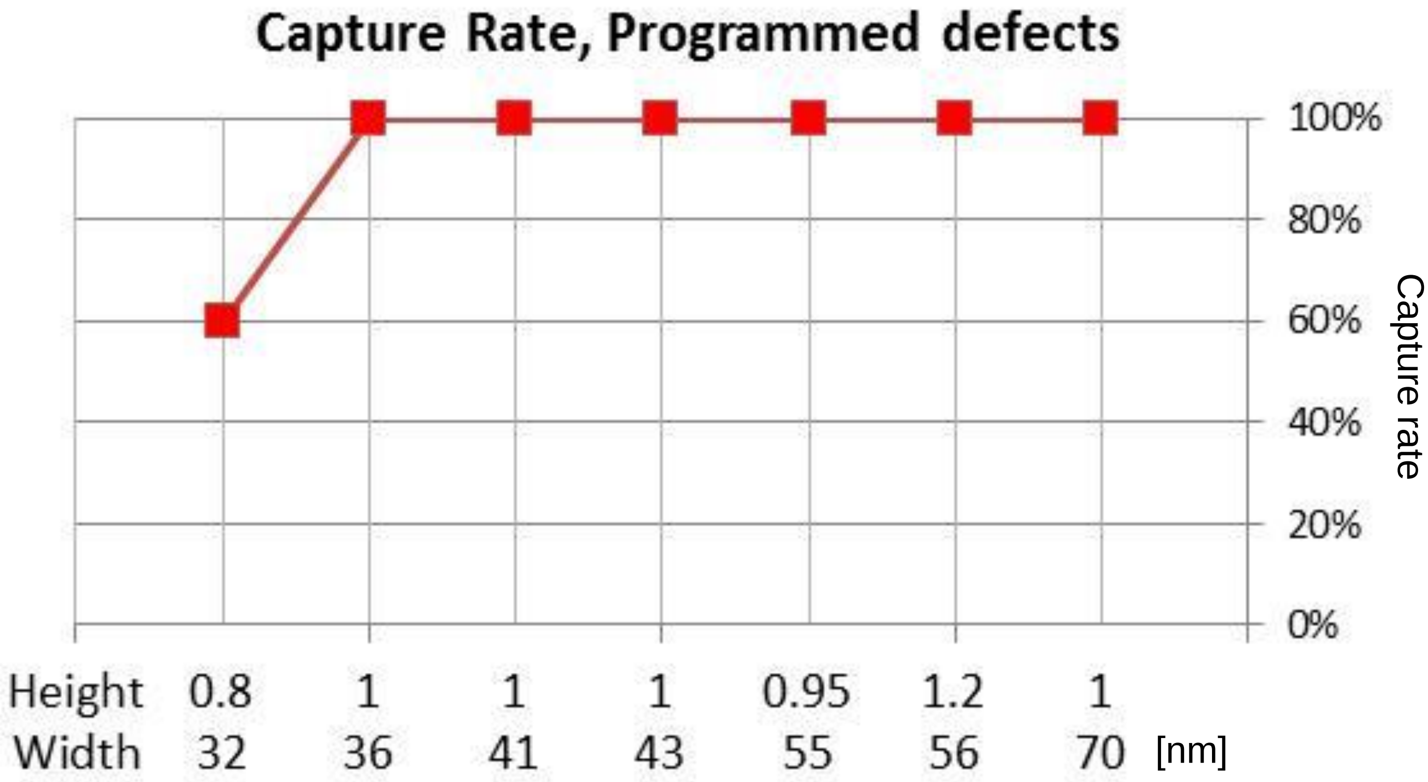

Defect sensitivity of the HVM ABI prototype for 16 nm node was confirmed by the programmed defect evaluation

Motivation of this work

<u>This work</u>
Inspection capability of the HVM ABI prototype for ‘native’ defect on actual mask blanks was evaluated

- Mask blanks were inspected by the HVM ABI prototype and an optical inspection tool
- Native defects detected by ABI were observed with AFM and wafer impact of them was evaluated with simulation
- Native defects not detected by ABI were observed with AFM ArF microscope and SEM and analyzed with EDX, and also wafer impact of them was evaluated with simulation
- Readiness of ABI for 16 nm node was discussed

Outline

1. Introduction
2. **Defects detected by ABI**
3. Not detected defects by ABI
4. Summary

Experiment

Inspection by ABI

- Mask blanks were inspected with the HVM ABI prototype
- Defects detected stably (detected in all of 3 times inspection or indicated sufficient signal intensity for one inspection) were selected
- Punch marks were created near the selected defects

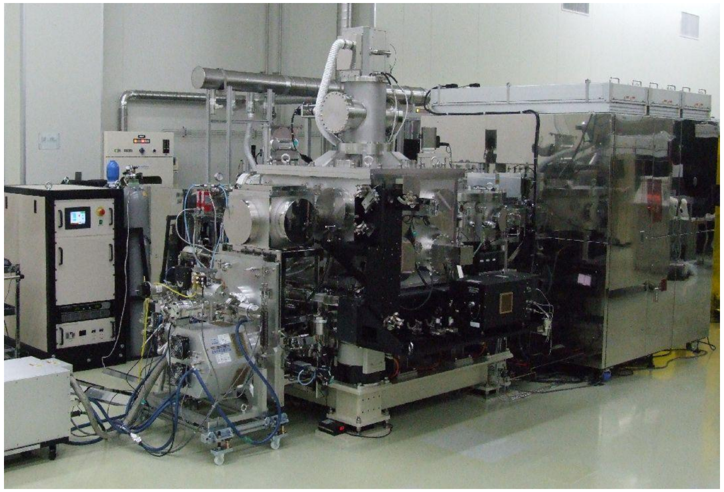

AFM measurement

- The selected defects were observed by AFM
- Defect dimensions were measured

  Height / depth : peak / valley to background

  Width: average of vertical and horizontal FWHMs

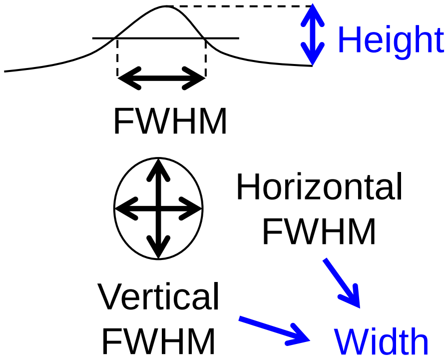

Distribution of defect dimensions detected by ABI was obtained

Simulation

Defect signal intensity of ABI

Dimensions of phase defects where signal intensities were the same as 1 nm-high 36 nm-wide defect were calculated

Defect dimensions detected at 100 % capture rate by ABI were obtained

Conformal structure

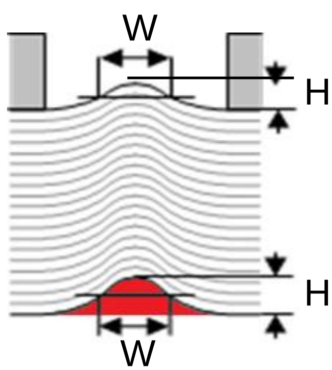

Wafer impact

Wafer impact of phase defects for 16 nm node was evaluated with variation of defect dimensions

Exposure condition
NA 0.33, Dipole (σ=0.4/0.8, open angle 90 deg.)
Defocus range +/-75 nm

A defect caused 10 % CD deviations → Printable

Phase defect

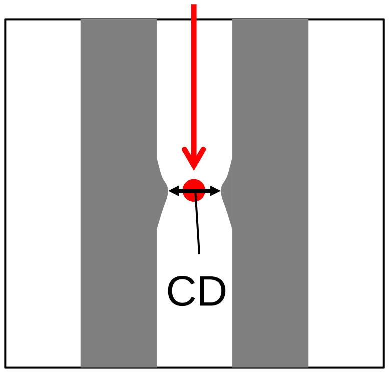

16 nm L/S pattern

Defect dimensions printable for 16 nm node was obtained

Distribution of detected defect dimension

Using the dimension of defects detected by ABI, distribution of defect dimension was obtained

$$\text{*) Detection density} = \frac{\text{Detection number in a certain range of dimension}}{\text{Total detection number}}$$

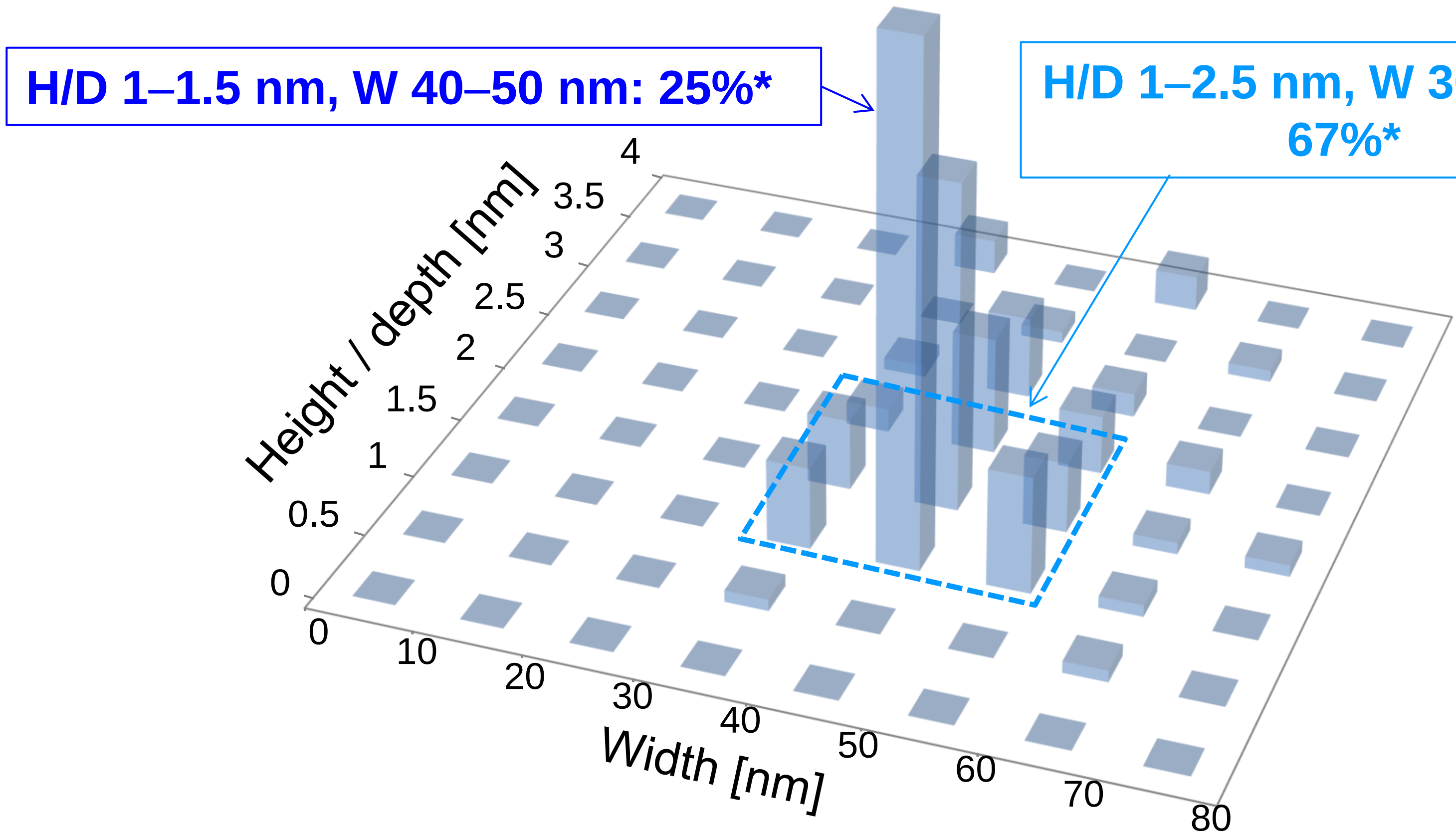

1-1.5 nm-high/deep 40-50 nm-wide defects were the most detected

ABI detectable and printable phase defects

Using simulation, dimensions of the ABI detectable and printable defects were obtained, and compared with the distribution of defect dimensions

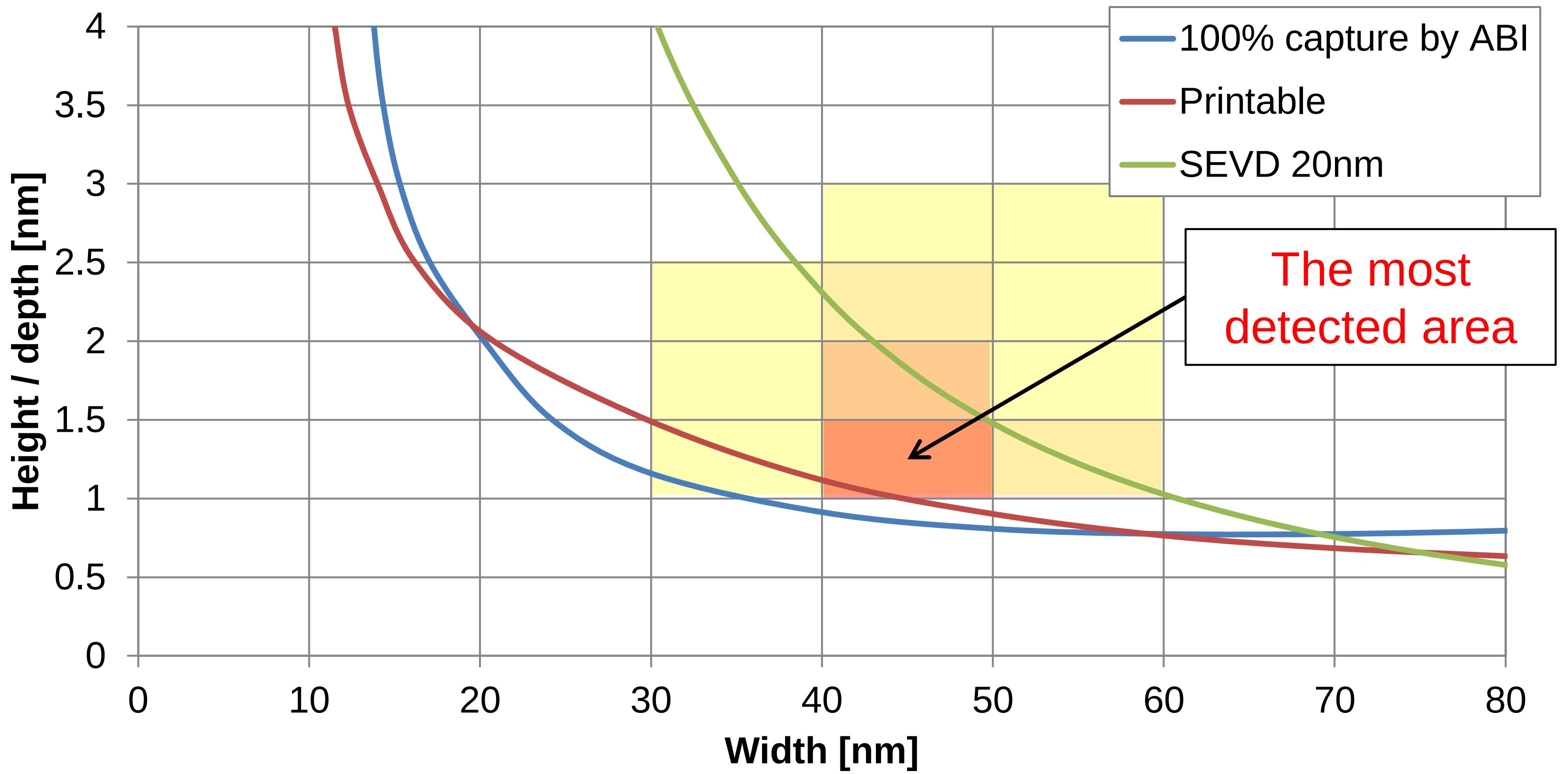

- ✓ Existing printable phase defects were detected by ABI at almost 100 %
- ✓ Defect dimensions in the most detected area were 20 nm and smaller in SEVD

Detection density vs. SEVD

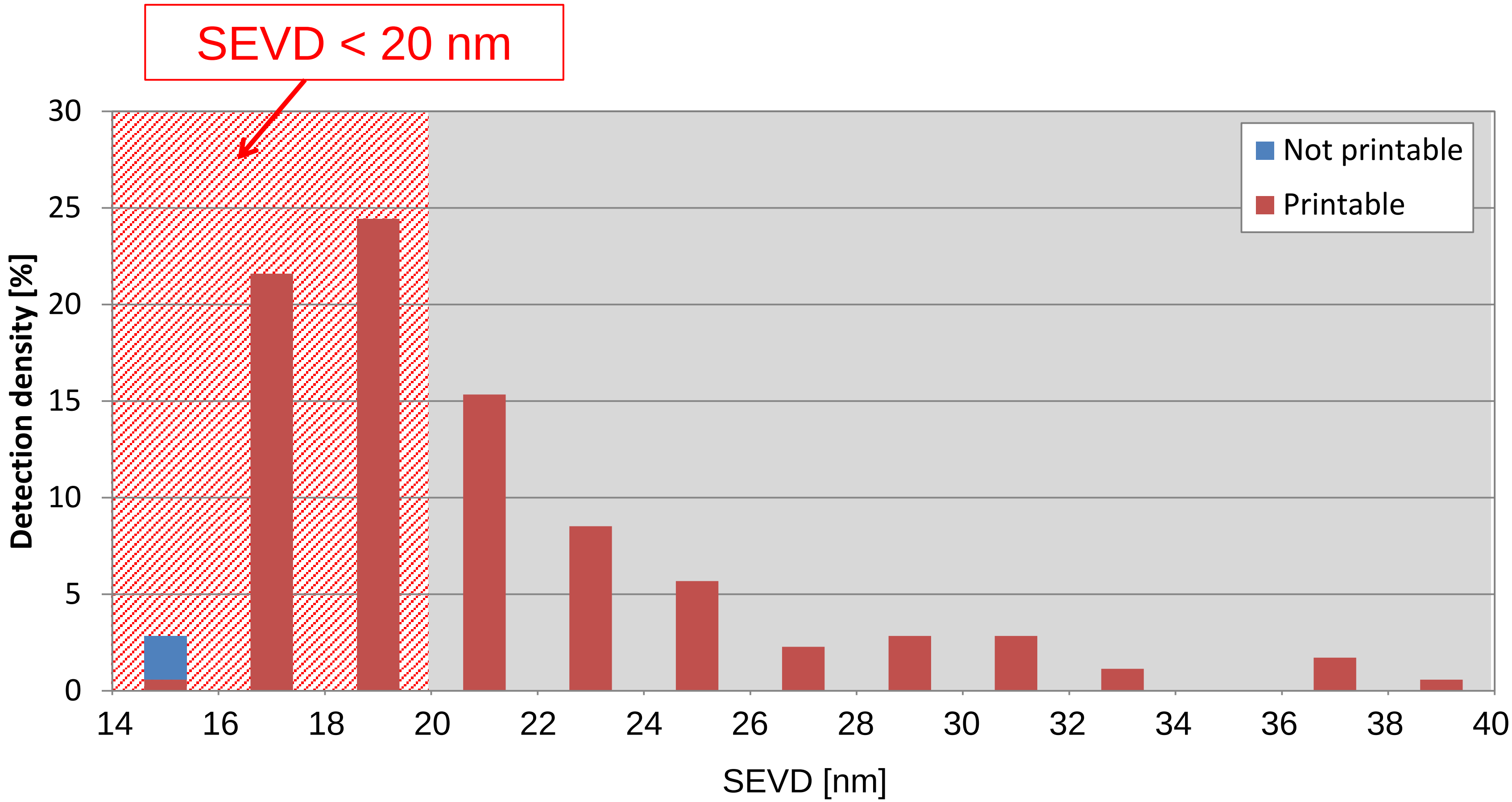

46 % of printable defects was smaller than 20 nm in SEVD

Outline

1. Introduction
2. Defects detected by ABI
3. **Not detected defects by ABI**
4. Summary

Not detected phase defect by ABI

ABI and optical inspection

Defects not-detected by ABI were collected

Among the not-detected defects, phase defects were extracted using AFM, ArF microscope and SEM and EDX

Not-detected but printable phase defects were extracted

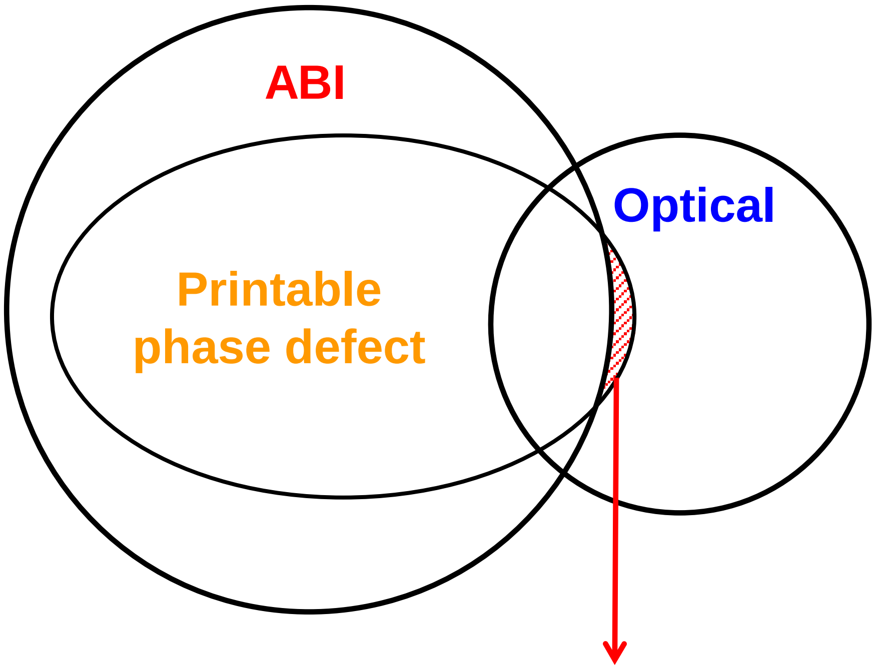

- ✓ < 1 % of the total detection*
- ✓ Aspect ratio（H or D / W) < 1/100

*) Total detection = ABI (defects detected 3 times) **U** Optical inspection

ABI signal intensity and wafer impact of low aspect phase defects were calculated with simulation

Measures to detect a low aspect defect

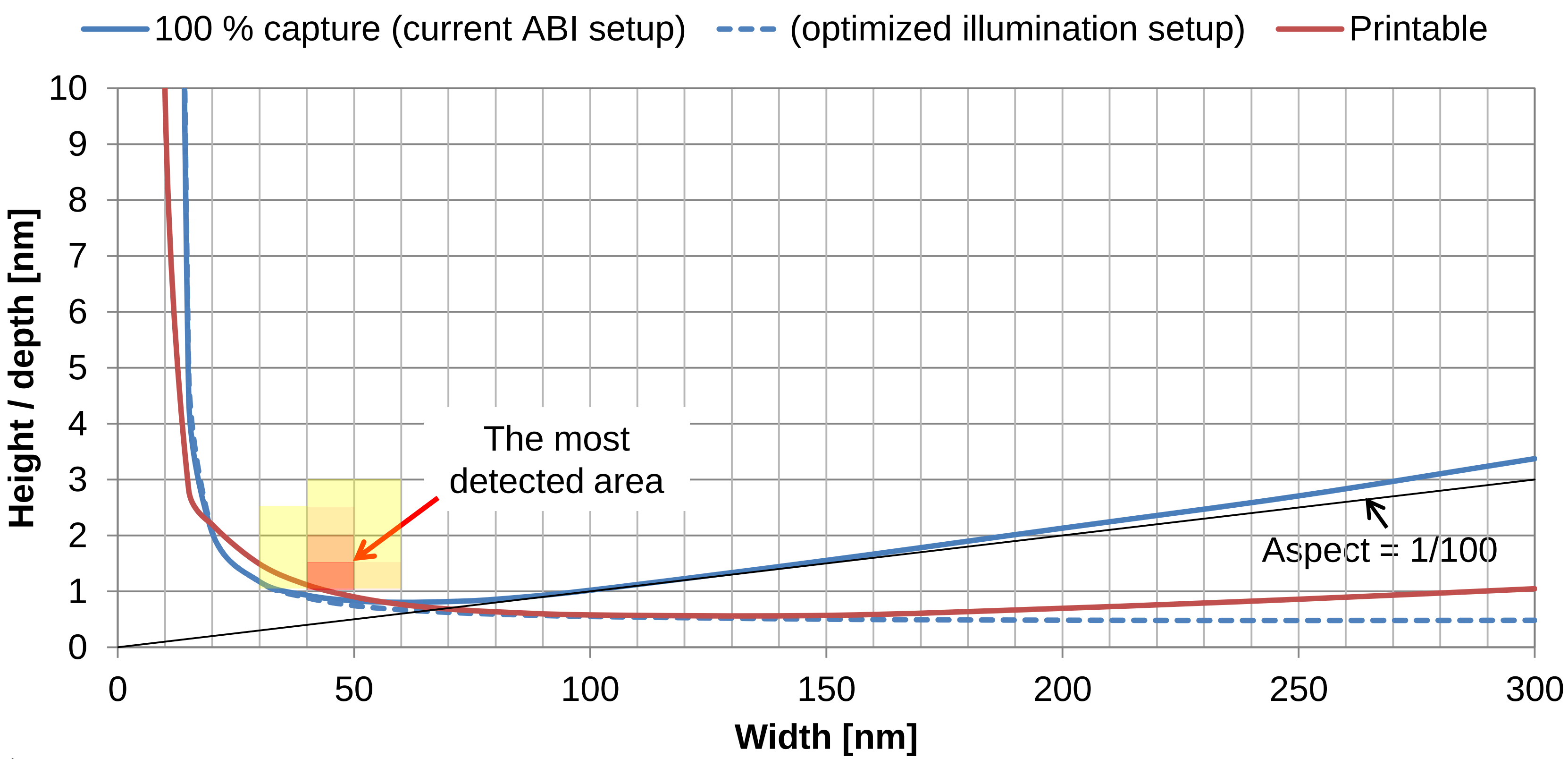

- ✓ Because defect dimensions where aspect ratio was lower than 1/100 were far from the concentrated defect area, it was hardly existed.
- ✓ The simulation result shows that a printable phase defect where aspect ratio was lower than 1/100 was not detected by ABI
- ✓ The optimized illumination setup enables to detect a low aspect but printable phase defect

Outline

1. Introduction
2. Defects detected by ABI
3. Not detected defects by ABI
4. **Summary**

Summary

- Existing printable defects were detected by ABI at almost 100 % capture rate.
- Almost the half of printable defects was smaller than 20 nm in SEVD. The ABI could detect such a small but printable phase defect.
- Although a printable phase defect where aspect ratio was lower than 1/100 was hardly existed, it was not detected by ABI
- The simulation result shows that optimization of the ABI illumination setup enables to detect a low aspect but printable phase defect.

Acknowledgement

This work was supported by New Energy and Industrial Technology Development Organization (NEDO) and Japan Ministry of Economy, Trade and Industry (METI)

Experiments were assisted by Kenji Sakamoto, EIDEC